# Growth inhibitory effects of celecoxib in human umbilical vein endothelial cells are mediated through $G_1$ arrest via multiple signaling mechanisms

**Ho-Pi Lin, Samuel K. Kulp, Ping-Hui Tseng, Ya-Ting Yang, Chi-Cheng Yang, Chang-Shi Chen, and Ching-Shih Chen**

**Division of Medicinal Chemistry and Pharmacognosy, College of Pharmacy, The Ohio State University, Columbus, Ohio**

## Abstract

**Evidence suggests that the angiogenic endothelium represents an important target through which celecoxib mediates *in vivo* antitumor effects. Nevertheless, the pharmacologic basis for celecoxib-caused growth inhibition in endothelial cells *in vitro* remains to be defined. Previously, we showed that celecoxib-induced apoptosis in PC-3 prostate cancer cells was mediated in part through the inhibition of 3-phosphoinositide-dependent kinase-1/Akt signaling. Our present findings show that celecoxib inhibits the growth of human umbilical vein endothelial cells (HUVEC) with pharmacologic profiles reminiscent of those of PC-3 cells. The underlying antiproliferative mechanism, however, may differ between these two cell types considering differences in the functional status of many tumor suppressors, including PTEN, p53, and retinoblastoma, all of which play integral roles in regulating cell cycle progression and survival. From a mechanistic perspective, the genomic integrity of the HUVEC system presents a vastly different intracellular context to examine how celecoxib acts to induce growth inhibition. Here, we obtain evidence that the antiproliferative effects of celecoxib and its close, cyclooxygenase-2-inactive analogue 4-[5-(2,5-dimethylphenyl)-3(trifluoromethyl)-1*H*-pyrazol-1-yl]benzenesulfonamide (DMC) in HUVECs at pharmacologically attainable concentrations (10–20 μmol/L) are attributable to the inhibition of phosphoinositide-dependent kinase-1/Akt signaling and cyclin-dependent kinase. Especially, celecoxib- and DMC-mediated $G_1$ arrest is associated with attenuated retinoblastoma phosphorylation through the inhibition of multiple cyclin-dependent kinases ($IC_{50}$, 10–35 μmol/L). Moreover, both celecoxib and DMC reduce neovascularization in the chicken chorioallantoic membrane assay, suggesting the involvement of a cyclooxygenase-2-independent mechanism in the *in vivo* antiangiogenic effects of celecoxib. [Mol Cancer Ther 2004;3(12):1671–80]**

## Introduction

An abundance of data from epidemiologic, preclinical, and clinical studies has firmly established cyclooxygenase-2 (COX-2) as a viable target for cancer prevention and therapy (1–3). The delineation of the malignant epithelium as a cellular target for COX-2 inhibition is based on the expression of COX-2 mRNA and protein in a wide variety of human epithelial malignancies (4–13). COX-2, however, is also expressed in the tumor microvasculature, indicating an angiogenic role for COX-2-derived prostaglandins in the support of tumor growth and suggesting the tumor stroma as a target for COX-2 inhibition (14, 15). In support of this view, it was shown that host cell COX-2 was important for xenograft tumor vascularization and growth, and COX-2-null stromal cells exhibited a diminished capacity to produce vascular endothelial growth factor (16). In addition, Masferrer et al. elegantly showed that the COX-2 inhibitor celecoxib was capable of inhibiting the growth of colon and lung xenograft tumors despite the restriction of COX-2 expression to the tumor-associated vasculature and its absence from the tumor cells themselves (15, 17). Together, these findings suggest that the well-established antitumor effects of celecoxib are at least in part mediated by inhibitory effects on the angiogenic endothelium.

Nonetheless, information regarding the mechanism underlying celecoxib-mediated growth inhibition in angiogenic endothelial cells is fragmentary vis-à-vis cancer cells in the literature. At the cellular level, celecoxib inhibits COX-2, causes cell cycle arrest, and induces apoptosis at different effective concentrations. However, the effects on cell cycle progression and apoptosis in cancer cell systems *in vitro* require concentrations that are several orders of magnitude greater than that required to inhibit COX-2 activity (i.e., tens of micromolar concentrations versus 0.04 μmol/L). Such findings are among a growing body of evidence that celecoxib mediates the antitumor effects via both COX-2-dependent and COX-2-independent mechanisms (16, 18–24). Among several non-COX-2 targets proposed for celecoxib, suppression of Akt through the inhibition of phosphoinositide-dependent kinase-1 (PDK-1) is particularly noteworthy (24, 25). As dysregulated PDK-1/Akt signaling plays a key role in promoting cancer cell proliferation and survival (13, 26), its inhibition represents

Received 5/5/04; revised 9/3/04; accepted 10/18/04.

**Grant support:** NIH grant CA-94829.

The costs of publication of this article were defrayed in part by the payment of page charges. This article must therefore be hereby marked advertisement in accordance with 18 U.S.C. Section 1734 solely to indicate this fact.

**Requests for reprints:** Ching-Shih Chen, Division of Medicinal Chemistry and Pharmacognosy, College of Pharmacy, Ohio State University, 336 Parks Hall, 500 West 12th Avenue, Columbus, OH 43210-1291. Phone: 614-688-4008; Fax: 614-688-8556. E-mail: chen.844@osu.edu

a major mechanism underlying celecoxib-mediated antitumor effects (19, 27). The unique ability of celecoxib to inhibit PDK-1, however, is not observed with other COX-2 inhibitors examined, such as rofecoxib, despite that they exhibit comparable COX-2 inhibitory potency (28, 29).

As Akt also plays a role in endothelial cell proliferation and survival (30), these findings raise a question of whether the growth inhibitory effects of celecoxib on the tumor vascular endothelium (15, 17) involve the inhibition of PDK-1/Akt signaling. To address this issue, we used human umbilical vein endothelial cells (HUVEC) as a model of the angiogenic endothelium to compare the growth inhibitory effects of celecoxib vis-à-vis a close, COX-2-inactive derivative of celecoxib. 4-[5-(2,5-Dimethylphenyl)-3(trifluoromethyl)-1*H*-pyrazol-1-yl]benzenesulfonamide (DMC), although devoid of COX-2 inhibitory activity (31), retains the ability to induce apoptosis in PC-3 prostate cancer cells through the inhibition of PDK-1/Akt signaling (20, 24). Our present findings show that both celecoxib and DMC inhibited HUVEC growth with pharmacologic profiles reminiscent of those in PC-3 cells. The mechanism underlying celecoxib-mediated growth inhibition may differ between these two types of cells because of differences in signaling mechanisms governing cell cycle progression and apoptosis. For example, PC-3 cells are deficient in the expression of tumor suppressors such as PTEN, p53, and retinoblastoma. From a mechanistic perspective, the genomic integrity of the HUVEC system presents a vastly different intracellular context to examine how celecoxib acts to induce growth inhibition. Here, we obtain evidence that the antiproliferative effects of celecoxib in HUVECs and DMC at pharmacologically attainable concentrations (i.e., $\leq$20 μmol/L) are attributable to $G_1$ arrest through the concurrent inhibition of PDK-1/Akt signaling and cyclin-dependent kinases (CDKs).

## Materials and Methods

### Reagents

DMC is a close structural analogue of celecoxib, of which the 5-aryl moiety is altered by replacing the 4-methylphenyl with a 2,5-dimethylphenyl function. This slight modification abrogated the activity of DMC in COX-2 inhibition ($IC_{50}$ > 100 μmol/L; ref. 31); however, its ability to block Akt phosphorylation and to induce apoptosis in cancer cells was retained (32). The synthesis of DMC has been described previously (31, 32). Celecoxib and rofecoxib were prepared from commercial Celebrex and Vioxx capsules by solvent extraction followed by recrystallization. For *in vitro* studies, these agents at various concentrations were dissolved in DMSO, and the final DMSO concentration was kept at 0.1% after addition to medium. Recombinant CDK1/cyclin B and CDK2/cyclin E complexes were purchased from Upstate, Inc. (Charlottesville, VA). Histone H1, indomethacin, and roscovitine were obtained from Sigma-Aldrich, Corp. (St. Louis, MO), and retinoblastoma substrate peptide was purchased from Panvera, Inc. (Madison, WI). Primary antibodies specific for the following proteins were purchased from the indicated vendors: cyclins A, B1, D1, and E, CDKs 2, 4, and 6, $p21^{Cip1}$, $p27^{Kip1}$, and extracellular signal-regulated kinase (ERK) from Santa Cruz Biotechnology, Inc. (Santa Cruz, CA); phospho-ERK and phospho-$Thr^{160}$ CDK2 from Cell Signaling Technology, Inc. (Beverly, MA); and poly(ADP-ribose)polymerase (PARP) from BD Biosciences PharMingen (San Diego, CA); CDK1 from Transduction Laboratories (Lexington, KY); and β-actin from ICN Biomedicals, Inc. (Costa Mesa, CA).

### Cell Culture

HUVECs were purchased from Glycotech, Inc. (Gaithersburg, MD) and were cultured in Medium 200 (Cascade Biologics, Portland, OR) supplemented with low-serum growth supplement (Cascade Biologics) at 37°C in a humidified $CO_2$ incubator. Final concentrations of the following components in the medium were 2% fetal bovine serum, 1 μg/mL hydrocortisone, 10 ng/mL human epidermal growth factor, 3 ng/mL basic fibroblast growth factor, and 10 μg/mL heparin. All experiments were done with cells between passages 3 and 7. For the drug treatment of HUVECs, test compounds were added in the presence of the low-serum growth supplement (Cascade Biologics). Jurkat T cells, used as the source for preparing the CDK4 immune complex, were purchased from American Type Culture Collection (Manassas, VA). The cells were cultured in RPMI 1640 supplemented with 10% fetal bovine serum at 37°C in a humidified $CO_2$ incubator.

### Growth Inhibition Assay

The assay was carried out according to a slight modification of the procedure suggested by the National Cancer Institute Angiogenesis Resources Center.[1] HUVECs were plated into 96-well plates at $1.5 \times 10^3$ cells per well in 100 μL of the aforementioned medium. After 24 hours (day 0), the test compound in 100 μL of the same medium was added to each well at twice the desired concentration. On day 0, one plate was stained with 0.5% crystal violet in 20% methanol for 10 minutes, rinsed with water, and air-dried. The remaining plates were incubated at 37°C for 72 hours, stained with 0.5% crystal violet in 20% methanol, rinsed with water, and air-dried. The crystal violet stain was eluted with a mixture of ethanol-0.1 mol/L sodium citrate (1:1), and absorbance at 540 nm was measured with an ELISA reader (Dynatech Laboratories, Chantilly, VA). Day 0 absorbance was subtracted from the absorbance values of the 72-hour samples, and data were plotted as percentage of control proliferation (vehicle-treated cells) to calculate $IC_{50}$ values (drug concentrations that cause 50% inhibition).

### Apoptosis Analysis

Two methods were used to assess drug-induced apoptotic cell death: detection of DNA fragmentation by the Cell Death Detection ELISA kit (Roche Diagnostics, Mannheim, Germany) and Western blot analysis of PARP cleavage. The ELISA was based on the quantitative determination of

[1] http://dtp.nci.nih.gov/aa-resources/aa_index.html

cytoplasmic histone-associated DNA fragments in the form of mononucleosomes or oligonucleosomes generated in the course of apoptotic death. In brief, $1.5 \times 10^6$ HUVECs were cultured in a T-75 flask for 24 hours before treatment. Cells were treated with the DMSO vehicle or the test agent at the indicated concentrations for indicated intervals and were collected, and cell lysates equivalent to $10^4$ cells were used in the ELISA. For the PARP cleavage assay, drug-treated cells were collected, washed with ice-cold PBS, and resuspended in lysis buffer containing 20 mmol/L Tris-HCl (pH 8), 137 mmol/L NaCl, 1 mmol/L $CaCl_2$, 10% glycerol, 1% NP40, 0.5% deoxycholate, 0.1% SDS, 100 μmol/L 4-(2-aminoethyl)benzenesulfonyl fluoride, 10 μg/mL leupeptin, and 10 μg/mL aprotinin. Soluble cell lysates were collected after centrifugation at 10,000 × *g* for 5 minutes. Equivalent amounts of proteins (60–100 μg) from each lysate were resolved in 10% SDS-PAGE. Bands were transferred to nitrocellulose membranes. Western blotting with an anti-PARP antibody was carried out, and apoptosis was detected by monitoring proteolysis of the 116-kDa native PARP enzyme to the apoptosis-specific 85-kDa fragment.

### Flow Cytometry for Cell Cycle Analysis

A detergent-trypsin method was used for the preparation of nuclei for flow cytometric DNA analysis (33). In brief, HUVECs were treated with DMSO or the test agent at the indicated concentration for 24 hours. The harvested cells ($1 \times 10^6$) were suspended in 400 μL of 40 mmol/L citrate buffer (pH 7.6), containing 250 mmol/L sucrose and 10% DMSO, and stored at −80°C until analysis. The cells were centrifuged and resuspended in 500 μL solution A (3.4 mmol/L trisodium citrate, 0.5 mmol/L Tris, 0.1% NP40, and 1.5 mmol/L spermine tetrahydrochloride with final pH 7.4) containing 15 μg/mL trypsin and 10 μg/mL EDTA. After incubating at 37°C for 30 minutes, 500 μL solution B, containing 0.5 mg/mL trypsin inhibitor and 0.1 mg/mL DNase-free RNase A, was added. After another incubation at 37°C for 30 minutes, 500 μL solution C, containing 0.05 mg/mL propidium iodide and 1.2 mg/mL spermine tetrahydrochloride, was added and incubated on ice for 1 hour. Cell cycle phase distributions were determined on a FACScan flow cytometer (Beckman-Coulter, Mountain View, CA).

### Akt Kinase Assay

Akt kinase assay was carried out according to a modified published procedure (34). Briefly, HUVECs were treated with DMSO vehicle or the test agents at the indicated concentrations for 12 hours, lysed, and homogenized in lysis buffer [50 mmol/L Tris-HCl (pH 7.5), 120 mmol/L NaCl, 1% (v/v) NP40, 1 mmol/L EDTA, 50 mmol/L NaF, 40 mmol/L β-glycerophosphate, and 1 μg/mL each of aprotinin, pepstatin, and leupeptin]. Cell lysates were centrifuged at 13,000 × *g* for 10 minutes, and the supernatants were collected for the kinase assay. Protein concentrations in the supernatants were determined by the Bradford method (Bio-Rad, Hercules, CA). The kinase assay was done by adding 10 μL substrate peptide (RPRAATF; ~80 μmol/L final assay concentration) and 10 μL [γ-$^{32}$P]ATP (1 mCi/mL) to equivalent amounts of supernatant (20 μg of total protein). After incubation for 30 minutes at 30°C, 25 μL of each reaction mixture were slowly spotted onto P81 phosphocellulose paper. After three washes with 0.75% phosphoric acid, the papers were transferred to scintillation vials containing 5 mL liquid scintillation cocktail. Radioactivity was measured in a scintillation counter.

### Transient Transfection by Calcium Phosphate Coprecipitation Method

The constitutively active Akt construct HA-PKB-T308D/S473D was kindly provided by Dr. Brian Hemmings (Friedrich Miescher Institute, Basel, Switzerland). HUVECs were seeded into T-75 flasks ($1 \times 10^6$ per flask). Various amounts of the plasmid were added to 450 μL TE buffer [10 mmol/L Tris-HCl, 1 mmol/L EDTA (pH 7.2)] followed by the addition of 50 μL of 2.5 mol/L $CaCl_2$ solution [10 mmol/L HEPES (pH 7.2)]. After briefly mixing the DNA-$CaCl_2$ solution, it was added dropwise to 500 μL of 2× HBS (280 mmol/L NaCl, 10 mmol/L KCl, 12 mmol/L dextrose, 50 mmol/L HEPES, and 1.5 mmol/L $Na_2HPO_4$). After 30 minutes of incubation, the mixture was applied to HUVECs directly. The calcium phosphate–containing medium was replaced by normal medium after 6 hours of incubation, and the transfected cells were harvested after additional 3 days for experiments.

### CDK1/Cyclin B Kinase Assay

The reagents used in this assay were prepared according to the manufacturer's instructions (Upstate, 14-450). Briefly, for each assay, 10 μL of assay dilution buffer [20 mmol/L MOPS (pH 7.2), 25 mmol/L β-glycerophosphate, 5 mmol/L EGTA, 1 mmol/L sodium orthovanadate, and 1 mmol/L DTT] containing the test agent at varying concentrations, 10 μL inhibitor cocktail (20 μmol/L protein kinase C inhibitor peptide, 2 μmol/L protein kinase A inhibitor peptide, and 20 μmol/L compound R24571), and 10 μL active CDK1/cyclin B (20 ng) were mixed and incubated for 15 minutes. Then, 10 μL of histone H1 (0.5 mg/mL) and 10 μL of diluted [γ-$^{32}$P]ATP solution were added to the mixture. After reacting at 30°C for 30 minutes, 25 μL of mixture were transferred to P81 paper. The paper was washed with 0.75% phosphoric acid thrice and acetone once and put into 5 mL scintillation cocktail. The radioactivity was measured by the scintillation counter.

### CDK2/Cyclin E Kinase Assay

The reagents used in this assay were prepared according to the manufacturer's instructions (Upstate, 14-475). Briefly, for each assay, 10 μL of reaction buffer [50 mmol/L MOPS (pH 7.0) and 2.5 mmol/L EDTA] containing the test agents at varying concentrations, and 2.5 μL of active CDK2/cyclin E (20 ng) were mixed and incubated for 15 minutes. Then, 2.5 μL of histone H1 (1 mg/mL) and 10 μL of diluted [γ-$^{32}$P]ATP solution were added into the mixture. After reacting at 30°C for 30 minutes, 20 μL of mixture were transferred to P81 paper. The paper was washed with 0.75% phosphoric acid thrice and acetone once and transferred to 5 mL scintillation cocktail. The radioactivity was measured by the scintillation counter.

### Immunoprecipitated Cyclin E Kinase Assay

Cyclin E immunoprecipitates were prepared from the lysates of HUVECs as follows. HUVECs were collected by scraping from T-75 flasks at 80% confluence and resuspended in lysis buffer [50 mmol/L Tris-HCl (pH 7.5), 120 mmol/L NaCl, 1% (v/v) NP40, 1 mmol/L EDTA, 50 mmol/L NaF, 40 mmol/L β-glycerophosphate, and 1 μg/mL each of aprotinin, pepstatin, and leupeptin]. After homogenization, the lysates were centrifuged at 13,000 × *g* for 10 minutes. The supernatants were collected and diluted with the same buffer at a 1:500 ratio. The diluted lysates were then subjected to immunoprecipitation at 4°C for 2 hours with antibodies (1:100) against cyclin E (Santa Cruz Biotechnology). Protein A-agarose beads were then added followed by an additional 1 hour of incubation at the same temperature. The beads with captured immune complexes were washed thrice with lysis buffer and used for the CDK2 kinase assay. The assay was done as described above for the CDK2/cyclin E kinase assay, except for the use of the cyclin E immunoprecipitates instead of the recombinant enzymes and the inclusion of a short centrifugation step to pellet the beads before transfer of supernatants to P81 paper.

### CDK4 Kinase Assay

CDK4 immunoprecipitates were prepared from the lysates of Jurkat T cells as follows. Jurkat T cells ($8 \times 10^8$) were lysed with lysis buffer [50 mmol/L Tris-HCl (pH 7.5), 120 mmol/L NaCl, 1% (v/v) NP40, 1 mmol/L EDTA, 50 mmol/L NaF, 40 mmol/L β-glycerophosphate, 0.1 mmol/L phenylmethylsufonyl fluoride, and 1 μg/mL each of aprotinin, pepstatin, and leupeptin] followed by homogenization and centrifugation at 13,000 × *g* for 10 minutes. The supernatant was incubated with anti-CDK4 antibodies (Santa Cruz Biotechnology) at 4°C for 2 hours followed by addition of protein A-agarose beads for 1 hour. The beads with captured immune complexes were washed thrice by lysis buffer and twice by CDK4 assay buffer [50 mmol/L MOPS (pH 7.0) and 2.5 mmol/L EDTA] and subjected to CDK4 kinase assay. In brief, 5 μL of assay buffer with test agent at the desired concentration and 25 μL of the same buffer containing CDK4 immunoprecipitates were incubated together for 15 minutes. Then, 10 μL of assay buffer containing retinoblastoma substrate peptide (2.5 ng) and 10 μL of diluted [$\gamma$-$^{32}$P]ATP solution were added into the mixture. The reaction mixture was incubated at 30°C for 1.5 hours followed by brief centrifugation. Thirty microliters of the supernatant were carefully transferred to P81 paper. The paper was washed thrice with 0.75% phosphoric acid followed by one wash with acetone and transferred to 5 mL scintillation cocktail. Radioactivity was measured by the scintillation counter.

### Quantitative Determination of pRb$^{Thr821}$ and Total Retinoblastoma in HUVECs

The levels of phosphorylated retinoblastoma and total retinoblastoma in cell lysates were determined using Human pRb$^{Thr821}$ ELISA kit and Human Total Rb ELISA kit, respectively (both from Biosource International, Camarillo, CA). HUVEC cells were seeded on 0.1% gelatin-coated T-75 flasks 1 day before treatments. The cells were treated with 20 μmol/L celecoxib or DMC or with DMSO vehicle for 24 or 72 hours. For the 24-hour treatment, cells were plated at a density of $1.5 \times 10^6$ cells per flask, with 12 flasks per treatment group. For the 72-hour treatment, cells were plated at a density of $8 \times 10^5$ cells per flask to avoid overconfluence, with 20 flasks per treatment group. Cells were harvested by scraping and treated with lysis buffer [50 mmol/L Tris-HCl (pH 7.5), 120 mmol/L NaCl, 1% NP40 (v/v), 1 mmol/L EDTA, 50 mmol/L NaF, 40 mmol/L β-glycerophosphate, 0.1 mmol/L phenylmethylsufonyl fluoride, and 1 mg/mL each of aprotinin, pepstatin, and leupeptin], briefly sonicated, and centrifuged at 13,000 × *g* for 25 minutes. The supernatants were collected for immediate analysis of pRb$^{Thr821}$ and total retinoblastoma contents by the immunoassays. The ELISAs were done according to the manufacturer's instructions.

### Western Blot Analysis of Signaling Components

Drug-treated cells were collected as described above, washed with PBS, resuspended in SDS-PAGE loading buffer [100 mmol/L Tris-HCl (pH 6.8), 4% (w/v) SDS, 0.2% (w/v) bromophenol blue, 20% (v/v) glycerol, and 200 mmol/L DTT], sonicated for 5 seconds, and boiled for 5 minutes. After brief centrifugation, equivalent amounts of soluble proteins, as determined by the Bradford method, were resolved in 8% to 15% SDS-polyacrylamide minigels, depending on the size of desired protein, and transferred to nitrocellulose membranes with the use of a semidry transfer cell (Bio-Rad). The membranes were washed twice with TBS [0.3% (w/v) Tris, 0.8% (w/v) NaCl, and 0.02% (w/v) KCl] containing 0.05% Tween 20 (TBST) and then incubated with TBS containing 5% nonfat dry milk for 20 minutes to block nonspecific antibody binding. Each membrane was then incubated at 4°C for 12 hours with a primary antibody specific for cyclins A, B1, D1, and E, CDKs 1, 2, 4, and 6, p21$^{Cip1}$, p27$^{Kip1}$, β-actin, ERK, or phospho-ERK, which was diluted 1:1,000 in TBS containing 1% nonfat dry milk. The membranes were washed twice with TBST and then incubated at room temperature for 1 hour with a horseradish peroxidase–conjugated goat anti-rabbit or anti-mouse immunoglobulin G diluted 1:5,000 in TBS containing 1% nonfat dry milk. The membranes were washed twice with TBST, and bound antibody was visualized by enhanced chemiluminescence Western blotting detection reagents (Amersham Pharmacia Biotech, Little Chalfont, United Kingdom). Unphosphorylated ERK2, as immunostained with anti-ERK2 antibodies, were used as internal standards for the comparison of phospho-ERK2 levels among samples of different exposure intervals.

### Chicken Chorioallantoic Membrane Assay

The chorioallantoic membrane (CAM) assay was done in accordance with procedures described by Marks et al. (35). Eight-day-old fertile White Leghorn chicken eggs were obtained from the Ohio State University Department of Animal Sciences and CBT Farms (Chestertown, MD). Eggs were candled to ensure fertility and viability of the

embryos before inclusion in the experiment. A small hole (~1 cm diameter) was made in the shell over the air sac through which treatment solutions were directly pipetted onto the surface of the CAM. Treatments included celecoxib, DMC, rofecoxib, indomethacin, and roscovitine, which were prepared as suspensions in PBS and applied to the CAM in a total volume of 15 μL containing 0.15, 1.5, or 15 nmol of drug. Controls received 15 μL PBS only. Each treatment group contained eight eggs. The holes were then sealed with Micropore surgical tape (3M Health Care, St. Paul, MN), and the eggs were incubated in a humidified egg incubator (Murray McMurray Hatcheries, Webster City, IA) at 37°C for 72 hours. After treatment, the area of each CAM to which the treatment agent had been applied was quickly excised and fixed in 4% paraformaldehyde (w/v in PBS). Images of the CAMs were acquired with a digital camera (Nikon Coolpix 990, Melville, NY) and visualized for quantitation of vascularity in Adobe Photoshop 6.0 software. Each digital CAM image was overlaid with a 1 × 1-cm grid, and the number of blood vessel branch points within the grid was counted. Vascular densities in the CAMs were expressed as a percentage of the blood vessel branch points in the vehicle-treated control CAMs. For determination of phospo-Akt status, CAMs treated with 15 nmol of DMC were excised after 24, 48 and 72 hours of treatment, quickly frozen in liquid nitrogen, and stored at −80°C until analysis. CAMs were homogenized in the previously described lysis buffer, and Western blot analysis was performed as described above.

## Results

### HUVEC Growth Is Inhibited by Celecoxib and DMC

We assessed the growth inhibitory effects of celecoxib vis-à-vis DMC and rofecoxib on HUVECs according to a

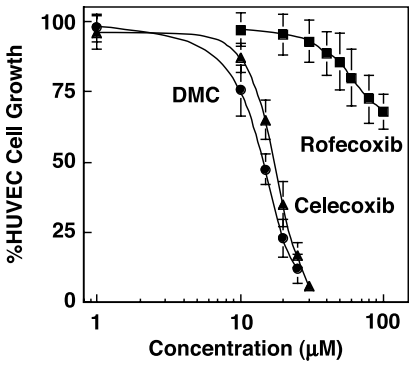


**Figure 1.** Dose dependency of the growth inhibitory effect of celecoxib, DMC, and rofecoxib in HUVECs. Cells were seeded into 96-well plates (1,500 cells per well) in six replicates in Medium 200 containing 2% fetal bovine serum, 1 μg/mL hydrocortisone, 10 ng/mL human epidermal growth factor, 3 ng/mL basic fibroblast growth factor, and 10 μg/mL heparin. After 24 hours of incubation, test agents were added at the indicated concentrations. After 72 hours of drug exposure, cells were stained with crystal violet, and cell viability was determined as described in Materials and Methods. Cell growth over the treatment period was expressed as a percentage of that in the vehicle (DMSO)-treated group. *Points,* mean; *bars,* SD. Experiments were done at least thrice.

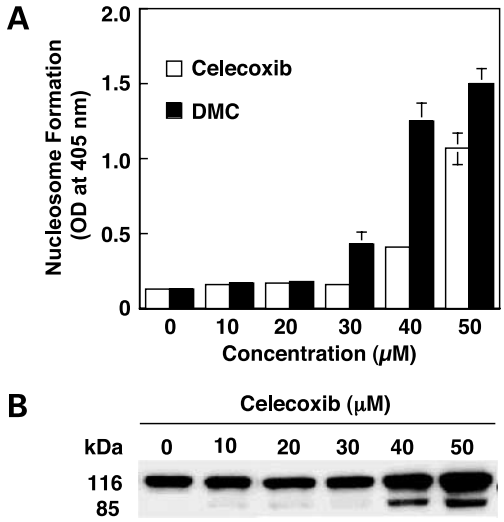


**Figure 2.** Dose-dependent effects of celecoxib and DMC on HUVEC apoptosis. HUVECs were exposed to varying concentrations of celecoxib or DMC for 24 hours, under the conditions described in the legend of Fig. 1. **A,** quantitative measurement of the formation of nucleosomes by the Cell Death Detection ELISA. *Columns,* mean ($n$ = 3); *bars,* SD. **B,** induction of PARP cleavage by celecoxib. PARP proteolysis to the apoptosis-specific 85-kDa fragment was monitored by Western blotting.

National Cancer Institute standard procedure (Fig. 1). Among these three agents, celecoxib and DMC exhibited moderate potency in suppressing HUVEC growth, with $IC_{50}$ of 18 and 15 μmol/L, respectively. The concentration required to attain complete growth inhibition was ~30 μmol/L for both agents. In contrast, rofecoxib could only cause partial inhibition of HUVEC growth at concentrations exceeding 50 μmol/L. These data suggest that the *in vitro* growth inhibitory effects of celecoxib on HUVECs involved COX-2-independent mechanisms.

### Celecoxib and DMC Inhibit HUVEC Growth by Causing $G_1$ Arrest

Both agents exhibited significant inhibitory effects on the growth of HUVECs between 10 and 20 μmol/L. We obtained two lines of evidence that this growth inhibition was attributable to $G_1$ cell cycle arrest in lieu of apoptosis. First, examinations of DNA fragmentation and PARP cleavage in drug-treated HUVECs indicate that neither agent triggered apoptotic death at 20 μmol/L (Fig. 2). Second, cell cycle analyses show a dose-dependent accumulation of cells in the $G_0$-$G_1$ phase, accompanied by comparative decreases in the S and $G_2$-M fractions (Table 1). Relatively, DMC exhibited higher potency than celecoxib in causing $G_1$ arrest, which is consistent with that observed in cell growth.

### Celecoxib and DMC Mediate $G_1$ Arrest through the Inhibition of Multiple Signaling Targets

Celecoxib and DMC inhibit PDK-1 activity with $IC_{50}$ values of 48 and 38 μmol/L, respectively, thereby diminishing the activation of Akt (24). This effect is mediated by

**Table 1. Cell cycle phase distribution of HUVECs treated with celecoxib or DMC at the indicated concentrations in 2% fetal bovine serum – supplemented medium for 24 hours**

| | | Cells in Cell Cycle Phases (%) | | |
|---|---|---|---|---|
| | | $G_0$-$G_1$ | S | $G_2$-M |
| DMSO vehicle | | 53.3 ± 4.4 | 11.9 ± 0.8 | 33.7 ± 5.7 |
| Celecoxib (μmol/L) | 10 | 62.55 ± 5.7 | 9.56 ± 1.9 | 24.2 ± 4.7 |
| | 15 | 64.6 ± 4.0 | 9.4 ± 1.7 | 22.9 ± 3.0 |
| | 20 | 65.9 ± 3.9 | 8.6 ± 2.0 | 22.5 ± 3.0 |
| | 25 | 69.3 ± 3.8 | 6.3 ± 1.6 | 22.9 ± 3.2 |
| DMC (μmol/L) | 10 | 64.3 ± 4.1 | 8.5 ± 1.7 | 23.4 ± 3.4 |
| | 15 | 65.2 ± 3.6 | 7.8 ± 1.6 | 22.9 ± 3.5 |
| | 20 | 69.7 ± 7.1 | 6.1 ± 2.4 | 20.8 ± 3.1 |
| | 25 | 73.2 ± 3.0 | 4.2 ± 2.9 | 22.1 ± 1.5 |
| Rofecoxib (μmol/L) | 10 | 53.4 ± 4.0 | 10.5 ± 2.8 | 32.8 ± 0.7 |
| | 15 | 52.9 ± 3.2 | 11.7 ± 2.0 | 33.6 ± 2.7 |
| | 20 | 54.2 ± 3.7 | 10.9 ± 1.7 | 34.0 ± 2.3 |
| | 25 | 54.0 ± 3.2 | 11.2 ± 2.8 | 34.2 ± 1.8 |

NOTE: Control cells received DMSO vehicle. Each tabulated percentage represents the average of three independent experiments.

competition with ATP for its binding site on PDK-1 (36). We have observed previously that celecoxib- and DMC-induced blockade of Akt activation in PC-3 cells requires a lower concentration of each agent than that required to inhibit PDK-1 activity (24), a discrepancy that we attributed to the concomitant action of protein phosphatase 2A, which dephosphorylates activated Akt (37, 38). In contrast to PC-3 cells, HUVECs display very low levels of phospho-Akt due to the presence of functional PTEN (data not shown). Consequently, the mechanism underlying celecoxib-mediated cell cycle arrest in HUVECs might differ from that of PC-3 cells. To shed light onto this issue, we first examined the Akt kinase activity from HUVECs treated with celecoxib or DMC over a concentration range of 10 to 50 μmol/L (Fig. 3). In line with our observation in PC-3 cells (24), celecoxib or DMC treatment of HUVECs reduced intracellular Akt activity in a dose-dependent manner, with $IC_{50}$ values of 28 and 20 μmol/L, respectively.

To examine whether Akt played an obligatory role in celecoxib-mediated $G_1$ arrest, we transiently transfected HUVECs with varying levels of a plasmid encoding constitutively active Akt ($Akt^{T308D/S473D}$). This transient transfection resulted in a good correlation between the Akt kinase activity and the dose of plasmid DNA, resulting in 36% and 75% increases in Akt activity with 7.5 and 15 μg DNA per $10^6$ cells, respectively, as compared with mock transfection. However, cell cycle distribution in response to the treatment of 20 μmol/L celecoxib in transiently transfected cells was the same as that of the mock-transfected counterparts (data not shown), suggesting the existence of other cellular target(s) for celecoxib in HUVECs.

As celecoxib inhibits PDK-1 activity through ATP competition, a crucial issue that could shed light on alternative targets is the specificity of its kinase inhibition, particularly with respect to CDKs in light of their direct involvement in cell cycle progression. As CDKs phosphorylate retinoblastoma to enable cells to progress from $G_1$ to S phase (39, 40), we analyzed the phosphorylation status of retinoblastoma as an indicator of CDK activity in drug-treated HUVECs. Specifically, we evaluated the phosphorylation level of $Thr^{821}$, a preferential phosphorylation site for CDK2 (41), by ELISA following exposure of HUVECs to 20 μmol/L celecoxib or DMC for 24 and 72 hours. As shown in Fig. 4A, a time-dependent decrease in the ratio of $pRb^{Thr821}$ to total retinoblastoma was observed in both treatment groups. As intracellular CDK2 forms complexes with cyclin E and several cell cycle regulators such as $p21^{Cip1}$ and $p27^{Kip1}$ (42), we examined the effect of celecoxib and DMC on the CDK2 kinase activity of immunoprecipitated cyclin E from HUVECs (Fig. 4B). Both agents exhibited significant inhibitory activity on the cyclin E immune complexes with $IC_{50}$ of ~10 μmol/L.

This $IC_{50}$, however, was significantly lower than that determined with recombinant CDK2/cyclin E ($IC_{50}$: celecoxib, 26 μmol/L; DMC, 24 μmol/L). This discrepancy might be attributable to the presence of coregulators in the immune complex. Alternatively, CDK2 activity might also be modulated through $Thr^{160}$ phosphorylation by CDK2-activating kinase (43). Thus, we examined the $Thr^{160}$ phosphorylation status of CDK2 in HUVECs treated with 10 to 30 μmol/L celecoxib. As shown in Fig. 4C, celecoxib at these doses had no appreciable effect on the $Thr^{160}$ phosphorylation, excluding the involvement of CDK-activating kinase in celecoxib-mediated CDK2 inhibition.

In addition to CDK2, celecoxib and DMC also inhibited recombinant CDK1/cyclin B1 and CDK4 immune complexes. The estimated $IC_{50}$ values for celecoxib and DMC were 34 and 22 μmol/L for recombinant CDK1 and 16 and 14 μmol/L for the CDK4 immune complex, respectively.

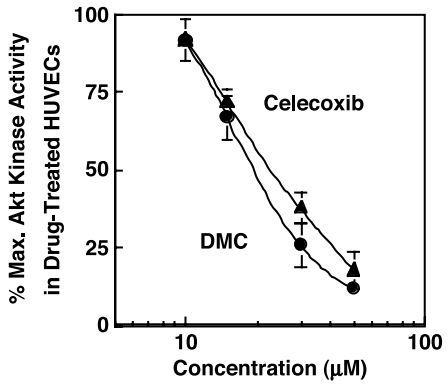


**Figure 3.** Dose-dependent effects of celecoxib and DMC on the kinase activity of Akt in drug-treated HUVECs. Cells were treated with the test reagent at the indicated concentrations for 2 hours in Medium 200 containing 2% fetal bovine serum, 1 μg/mL hydrocortisone, 10 ng/mL human epidermal growth factor, 3 ng/mL basic fibroblast growth factor, and 10 μg/mL heparin. Akt kinase activity in the cell lysates was analyzed as described in Materials and Methods. *Points,* mean ($n$ = 3); *bars,* SD.

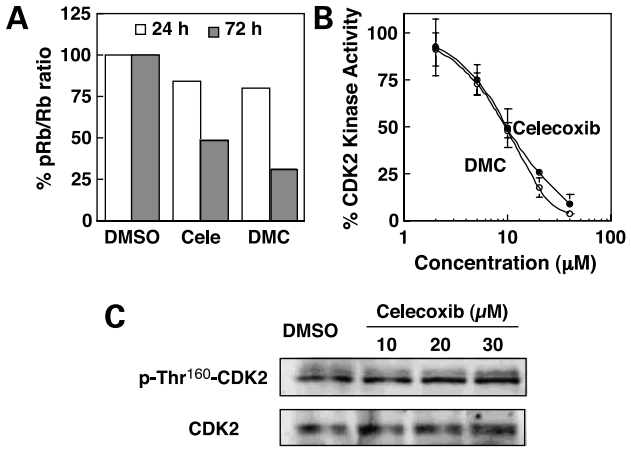


**Figure 4.** Effects of celecoxib and DMC on retinoblastoma (*Rb*) phosphorylation and CDK2 kinase activity of immunoprecipitated cyclin E complexes in HUVECs. **A,** time-dependent inhibition of $Rb^{Thr821}$ phosphorylation. HUVECs were treated with 20 μmol/L celecoxib (*Cele*) or DMC for 24 and 72 hours and were harvested for $pRb^{Thr821}$ and total retinoblastoma determinations by ELISA, respectively, as described in Materials and Methods. $pRb^{Thr821}$/total retinoblastoma ratio was determined and expressed as a percentage of the ratio in the vehicle (DMSO)–treated group. **B,** dose-dependent inhibition of the CDK2 kinase activity of immunoprecipitated cyclin E complexes. Cell lysates of HUVECs were treated with cyclin E antibodies, and the CDK2 kinase activity of the immune complex was analyzed as described in Materials and Methods. *Points,* mean ($n$ = 3); *bars,* SD. **C,** celecoxib at 10–30 μmol/L does not affect $Thr^{160}$ phosphorylation levels of CDK2, excluding the involvement of the CDK-activating kinase in inhibiting CDK2 kinase activity.

Earlier reports indicate that celecoxib mediated growth arrest by altering the expression levels of various cyclins or CDK inhibitors in different cancer cell systems (18, 21, 22, 44). In light of this transcriptional regulation, we examined the effect of celecoxib at 10, 20, and 30 μmol/L on the expression levels of various cell cycle regulatory proteins in HUVECs after 72 hours of exposure, which included cyclins A, B1, D1, and E, p21, p27, and CDKs 1, 2, 4, and 6 (Fig. 5A). However, celecoxib treatment did not alter the expression of any of these cell cycle regulatory proteins, which again suggests differences in signaling mechanisms governing celecoxib-mediated cell growth inhibition between cancer cells and HUVECs.

To examine whether celecoxib affected protein kinases other than PDK-1 and CDKs, it was submitted to a commercial kinase profiling service (Upstate) to assess its specificity in a panel of kinases, including Akt, CDK7/cyclin H, IκB kinase β, protein kinase A, $p70^{S6K}$, protein kinase C γ, mitogen-activated protein kinase kinase 1, mitogen-activated protein kinase 2, platelet-derived growth factor receptor α, c-RAF, and c-Src. However, none of these kinases was inhibited by 30 μmol/L celecoxib (data not shown).

We reported previously that treatment of PC-3 cells with 50 μmol/L celecoxib or DMC under serum-free conditions resulted in rapid dephosphorylation of ERK (45). However, within the growth inhibitory range of 10 to 30 μmol/L in medium containing 2% serum (as recommended by the HUVEC supplier, Cascade Biologics), neither agent caused an appreciable change in the level of phospho-ERKs in HUVECs (Fig. 5B). This finding suggests that ERK inhibition does not play a role in celecoxib-induced $G_1$ arrest under these conditions.

### Chicken Chorioallantoic Membrane Assay

The above *in vitro* data provided a rationale to examine the *in vivo* efficacy of celecoxib and DMC in the inhibition of neovascularization by using a CAM assay (Fig. 6). The CAMs of fertile 8-day-old White Leghorn chicken eggs were treated *in vivo* with 0.15, 1.5, or 15 nmol celecoxib or DMC suspended in 15 μL PBS. In addition, the COX-2 inhibitor rofecoxib, the nonselective COX inhibitor indomethacin, and the CDK inhibitor roscovitine were also examined for their *in vivo* antiangiogenic activities for comparison ($n$ = 8 for all treatment groups). Figure 6A shows that, in comparison with the untreated group, DMC reduced vascular densities in the CAMs at all levels tested. Meanwhile, celecoxib, rofecoxib, indomethacin, and roscovitine also caused a significant reduction in neovascularization but only at the highest dose ($P < 0.05$). This finding is in line with the reported effects of a nonsteroidal anti-inflammatory drug (NSAID) on angiogenesis (46) and suggests the involvement of CDKs in the antiangiogenic action of celecoxib and DMC.

Figure 6B shows images of representative CAMs after treatment with 15 nmol celecoxib or DMC, and Fig. 6C

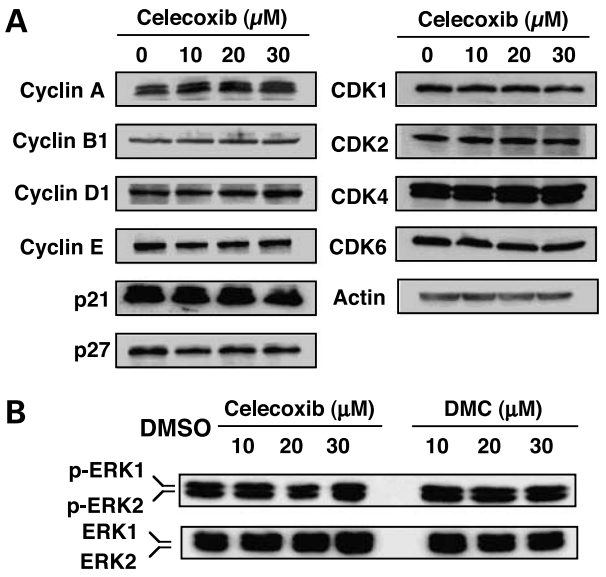


**Figure 5.** **A,** celecoxib at 10–30 μmol/L does not affect the expression levels of cyclins, cyclin-dependent inhibitors, and CDKs. HUVECs were treated with 10–30 μmol/L celecoxib for 72 hours followed by Western blot determination for indicated cell cycle regulatory proteins. β-Actin served as a loading control for each treatment. **B,** celecoxib and DMC at 10–30 μmol/L have no major impact on the phosphorylation status of ERKs. HUVECs were treated with both agents at the indicated concentrations for 24 hours. Western blot analyses for the respective phosphorylated and total proteins.

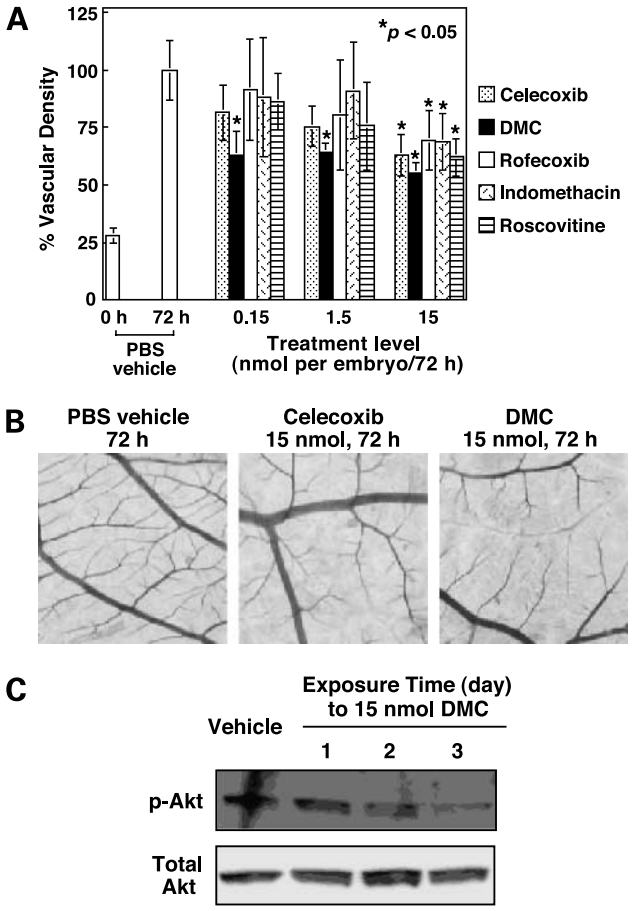


**Figure 6.** **A,** effect of celecoxib, DMC, rofecoxib, indomethacin, and roscovitine on neovascularization in the CAM assay. CAMs of fertile 8-day-old White Leghorn chicken eggs were treated the test agent at the indicated doses. After 72 hours, vascular densities in the CAMs were determined as described in Materials and Methods. Vascular densities in the CAMs were expressed as a percentage of that determined in the vehicle-treated control group. *Columns,* mean ($n$ = 8); *bars,* SD. **B,** images of representative CAMs after treatment with 15 nmol celecoxib or DMC for 72 hours. **C,** DMC-mediated inhibition of Akt phosphorylation in CAMs at different time intervals.

depicts a time-dependent decrease in phospho-Akt levels in CAMs after exposure to 15 nmol DMC, suggesting a link between Akt inhibition and the ability of DMC to block neovascularization.

## Discussion

Recent findings have identified the tumor endothelium as an important target for celecoxib-mediated antitumor effects *in vivo* (15, 17). The present study was aimed at exploring the pharmacologic basis that underlies the growth inhibitory effects of celecoxib in endothelial cells. Our use of DMC, a close structural analogue of celecoxib that lacks COX-2 inhibitory activity, permitted evaluation of the role of COX-2-independent mechanisms in the antiproliferative actions of celecoxib. In short, these findings indicate that celecoxib arrested the growth of HUVECs by acting on multiple non-COX-2 targets involved in the regulation of cell proliferation.

Both celecoxib and DMC induced $G_1$ arrest, in the absence of significant apoptosis, in HUVECs at concentrations up to 30 and 20 μmol/L, respectively. In contrast, rofecoxib required at least 50 μmol/L to exhibit appreciable inhibition. These findings suggest the involvement of COX-2-independent mechanisms in the antiproliferative action of celecoxib in HUVECs. These *in vitro* data were reflected in the results of the CAM assay in which both celecoxib and DMC reduced neovascularization. The *in vivo* efficacy of DMC seemed to be higher than that of celecoxib, which might be due to its slightly higher potency in inhibiting non-COX-2 targets or improved bioavailability due to increased hydrophobicity.

Beyond their utility as a model of the angiogenic endothelium, HUVECs provide an interesting contrast to the PC-3 prostate cancer cells in that they differ in many aspects of intracellular signaling. In contrast to HUVECs, PC-3 cells lack functional PTEN, p53, and retinoblastoma. Of particular interest is the loss of PTEN function in PC-3 cells, which results in elevated Akt signaling. Inhibition of PDK-1 and the consequent suppression of Akt activation by celecoxib cause growth inhibition and apoptosis in PC-3 cells. Consistent with our identification of PDK-1 as a major non-COX-2 target in PC-3 prostate cancer cells (24), Akt kinase activity was also suppressed in HUVECs treated with either celecoxib or DMC. However, enforced expression of constitutively active Akt kinase alone failed to abrogate celecoxib-mediated $G_1$ arrest, suggesting the involvement other targets in the HUVEC system.

Celecoxib has been shown to inhibit PDK-1 through the competition for ATP binding, a mechanism reminiscent to that of many other kinase inhibitors like flavopiridol and UCN-01. This mode of kinase inhibition, however, often gives rise to the cross-inhibition of related kinases. For example, flavopiridol, an inhibitor of several CDKs including CDK1, CDK2, CDK4, CDK6, and CDK7, was originally reported to inhibit epidermal growth factor receptor and protein kinase A at higher concentrations (47), and UCN-01 has been shown to inhibit $Ca^{2+}$-dependent protein kinase C, CDK1, CDK2, Chk1, and PDK-1 (47, 48). Our data indicate that celecoxib inhibited different CDKs with varying potency over a concentration range that was associated with $G_1$ arrest in HUVECs. Celecoxib at 30 μmol/L, however, did not affect the activity of a wide range of kinases examined, indicating the existence of a certain degree of specificity.

The ability of NSAIDs, including celecoxib, to compete for ATP binding sites has also been reported for several other non-COX-2 targets. Aspirin, sodium salicylate, sulindac, and sulindac sulfide have been shown to down-regulate nuclear factor-κB signaling by inhibiting IκB kinase β activity (49). For aspirin and sodium salicylate, this inhibition was attributed to the occupation of the ATP binding site. Our own work showed that

celecoxib inhibits endoplasmic reticulum $Ca^{2+}$-ATPases (19) and PDK-1 through competition for ATP binding (24). A similar mechanism was reported to mediate the inhibition of adenylyl cyclase by celecoxib with an $IC_{50}$ of 375 μmol/L (50). These findings underscore the pharmacologic complexity of the antiproliferative activities of celecoxib.

Whereas our findings show direct inhibition of CDK activity by celecoxib, others have reported indirect mechanisms. The intracellular elevation of the CDK inhibitors, $p21^{Cip1}$ and $p27^{Kip1}$, by celecoxib in several cancer types has been reported (18, 21, 22, 43). In the present study, similar effects on these proteins were not observed in celecoxib-treated HUVECs over the concentration range (10–30 μmol/L), which induced growth arrest without substantial apoptosis, and were lower than those used in the cited studies (≥50 μmol/L). A notable exception is the work of Narayanan et al. (21), which showed elevated expression levels of $p21^{Cip1}$ and $p27^{Kip1}$ after treatment with 10 and 20 μmol/L celecoxib in carcinogen-induced rat prostate cancer cells. In several glioblastoma cell lines, antiproliferative effects of celecoxib were attributed to the transcriptional down-regulation of cyclins A and B and the subsequent reduction in activities of corresponding CDKs in the absence of significant elevations in $p21^{Cip1}$ and $p27^{Kip1}$ (23). In our study, reductions in cyclin A or B1 were not observed with the concentration range we examined (Fig. 5). These discrepancies may result from differences in the concentrations of celecoxib used or differences in signaling pathways governing cell proliferation between cancer cells and HUVECs.

This study used HUVECs as a model to investigate the direct inhibitory effects of celecoxib on the angiogenic endothelium. Our findings show that celecoxib can induce growth arrest in these cells by interfering with multiple signaling molecules involved in the regulation of cell proliferation and suggest that its antiangiogenic activity in the tumor vasculature includes a role for COX-2-independent mechanisms. The results of the CAM assay are consistent with the report that the *in vivo* antiangiogenic actions of NSAIDs may involve both COX-2-dependent and COX-2-independent mechanisms (46). The relative contribution of COX-2 versus non-COX-2 mechanisms in the context of suppressing tumor-associated angiogenesis, however, is unclear and may vary with cell types or *in vivo* models. For instance, Masferrer et al. have elegantly shown the involvement of COX-2 inhibition in the antiangiogenic effect of celecoxib in a rat cornea model (15, 17). More recently, rofecoxib has also been shown to suppress microvessel density in human colorectal cancer liver metastases (51). In our CAM study, rofecoxib and indomethacin inhibited neovascularization but only at the highest dose used. A recent report indicates that the ability of indomethacin to inhibit angiogenesis also involved inhibition of ERK2 activity and interference with ERK nuclear translocation (46). These data further underscore the involvement of COX-2-independent signaling mechanisms in the antiproliferative activities of NSAIDs.

In summary, this study represents part of an emerging body of work that underscores the complexity of the pharmacologic actions of celecoxib. This complexity may confer broad anticancer efficacy and may underlie the established clinical value and potential of celecoxib. Meanwhile, the role of CDK inhibition in celecoxib-mediated antitumor effects in cancer cell systems (i.e., PC-3 cells) that lack functional retinoblastoma is currently under investigation.

## References


1. Marnett LJ, DuBois RN. COX-2: a target for colon cancer prevention. Annu Rev Pharmacol Toxicol 2002;42:55–80.
2. Turini ME, DuBois RN. Primary prevention: phytoprevention and chemoprevention of colorectal cancer. Hematol Oncol Clin North Am 2002;16:811–40.
3. Steinbach G, Lynch PM, Phillips RK, et al. The effect of celecoxib, a cyclooxygenase-2 inhibitor, in familial adenomatous polyposis. N Engl J Med 2000;342:1946–52.
4. Eberhart CE, Coffey RJ, Radhika A, Giardiello FM, Ferrenbach S, DuBois RN. Up-regulation of cyclooxygenase 2 gene expression in human colorectal adenomas and adenocarcinomas. Gastroenterology 1994;107:1183–8.
5. Sano H, Kawahito Y, Wilder RL, et al. Expression of cyclooxygenase-1 and -2 in human colorectal cancer. Cancer Res 1995;55:3785–9.
6. Soslow RA, Dannenberg AJ, Rush D, et al. COX-2 is expressed in human pulmonary, colonic, and mammary tumors. Cancer 2000;89:2637–45.
7. Hwang D, Scollard D, Byrne J, Levine E. Expression of cyclooxygenase-1 and cyclooxygenase-2 in human breast cancer. J Natl Cancer Inst 1998;90:455–60.
8. Gupta S, Srivastava M, Ahmad N, Bostwick DG, Mukhtar H. Overexpression of cyclooxygenase-2 in human prostate adenocarcinoma. Prostate 2000;42:73–8.
9. Kirschenbaum A, Klausner AP, Lee R, et al. Expression of cyclooxygenase-1 and cyclooxygenase-2 in the human prostate. Urology 2000;56:671–6.
10. Hida T, Yatabe Y, Achiwa H, et al. Increased expression of cyclooxygenase 2 occurs frequently in human lung cancers, specifically in adenocarcinomas. Cancer Res 1998;58:3761–4.
11. Tucker ON, Dannenberg AJ, Yang EK, et al. Cyclooxygenase-2 expression is up-regulated in human pancreatic cancer. Cancer Res 1999;59:987–90.
12. Zimmermann KC, Sarbia M, Weber AA, Borchard F, Gabbert HE, Schror K. Cyclooxygenase-2 expression in human esophageal carcinoma. Cancer Res 1999;59:198–204.
13. Cantley LC, Neel BG. New insights into tumor suppression: PTEN suppresses tumor formation by restraining the phosphoinositide 3-kinase/AKT pathway. Proc Natl Acad Sci U S A 1999;96:4240–5.
14. Form DM, Auerbach R. PGE2 and angiogenesis. Proc Soc Exp Biol Med 1983;172:214–8.
15. Masferrer JL, Leahy KM, Koki AT, et al. Antiangiogenic and antitumor activities of cyclooxygenase-2 inhibitors. Cancer Res 2000;60:1306–11.
16. Williams CS, Tsujii M, Reese J, Dey SK, DuBois RN. Host cyclooxygenase-2 modulates carcinoma growth. J Clin Invest 2000;105:1589–94.
17. Leahy KM, Ornberg RL, Wang Y, Zweifel BS, Koki AT, Masferrer JL. Cyclooxygenase-2 inhibition by celecoxib reduces proliferation and induces apoptosis in angiogenic endothelial cells *in vivo*. Cancer Res 2000;62:625–31.
18. Grosch S, Tegeder I, Niederberger E, Brautigam L, Geisslinger G. COX-2 independent induction of cell cycle arrest and apoptosis in colon cancer cells by the selective COX-2 inhibitor celecoxib. FASEB J 2001;15:2742–4.
19. Johnson AJ, Song X, Hsu A, Chen C. Apoptosis signaling pathways mediated by cyclooxygenase-2 inhibitors in prostate cancer cells. Adv Enzyme Regul 2001;41:221–35.

**20.** Johnson AJ, Hsu AL, Lin HP, Song X, Chen CS. The cyclooxygenase-2 inhibitor celecoxib perturbs intracellular calcium by inhibiting endoplasmic reticulum $Ca^{2+}$-ATPases: a plausible link with its anti-tumour effect and cardiovascular risks. Biochem J 2002;366:831–7.

**21.** Narayanan BA, Condon MS, Bosland MC, Narayanan NK, Reddy BS. Suppression of *N*-methyl-*N*-nitrosourea/testosterone-induced rat prostate cancer growth by celecoxib: effects on cyclooxygenase-2, cell cycle regulation, and apoptosis mechanism(s). Clin Cancer Res 2003; 9:3503–13.

**22.** Davis TW, O'Neal JM, Pagel MD, et al. Synergy between celecoxib and radiotherapy results from inhibition of cyclooxygenase-2-derived prostaglandin E2, a survival factor for tumor and associated vasculature. Cancer Res 2004;64:279–85.

**23.** Kardosh A, Blumenthal M, Wang WJ, Chen TC, Schonthal AH. Differential effects of selective COX-2 inhibitors on cell cycle regulation and proliferation of glioblastoma cell lines. Cancer Biol Ther 2004;3: 55–62.

**24.** Kulp SK, Yang YT, Hung CC, et al. 3-Phosphoinositide-dependent protein kinase-1/Akt signaling represents a major cyclooxygenase-2-independent target for celecoxib in prostate cancer cells. Cancer Res 2004;64:1444–51.

**25.** Arico S, Pattingre S, Bauvy C, et al. Celecoxib induces apoptosis by inhibiting 3-phosphoinositide-dependent protein kinase-1 activity in the human colon cancer HT-29 cell line. J Biol Chem 2002;277:27613–21.

**26.** Datta SR, Brunet A, Greenberg ME. Cellular survival: a play in three Akts. Genes Dev 1999;13:2905–27.

**27.** Zhu J, Song X, Lin HP, et al. Using cyclooxygenase-2 inhibitors as molecular platforms to develop a new class of apoptosis-inducing agents. J Natl Cancer Inst 2002;94:1745–57.

**28.** Waskewich C, Blumenthal RD, Li H, Stein R, Goldenberg DM, Burton J. Celecoxib exhibits the greatest potency amongst cyclooxygenase (COX) inhibitors for growth inhibition of COX-2-negative hematopoietic and epithelial cell lines. Cancer Res 2002;62:2029–33.

**29.** Kazanov D, Dvory-Sobol H, Pick M, et al. Celecoxib but not rofecoxib inhibits the growth of transformed cells *in vitro*. Clin Cancer Res 2004; 10:267–71.

**30.** Dimmeler S, Zeiher AM. Akt takes center stage in angiogenesis signaling. Circ Res 2000;86:4–5.

**31.** Penning TD, Talley JJ, Bertenshaw SR, et al. Synthesis and biological evaluation of the 1,5-diarylpyrazole class of cyclooxygenase-2 inhibitors: identification of 4-[5-(4-methylphenyl)-3-(trifluoromethyl)-1*H*-pyrazol-1-yl]benzenesulfonamide (SC-58635, celecoxib). J Med Chem 1997;40: 1347–65.

**32.** Song X, Lin HP, Johnson AJ, et al. Cyclooxygenase-2, player or spectator in cyclooxygenase-2 inhibitor-induced apoptosis in prostate cancer cells. J Natl Cancer Inst 2002;94:585–91.

**33.** Vindelov LL, Christensen IJ, Nissen NI. A detergent-trypsin method for the preparation of nuclei for flow cytometric DNA analysis. Cytometry 1983;3:323–7.

**34.** Bozinovski S, Cristiano BE, Marmy-Conus N, Pearson RB. The synthetic peptide RPRAATF allows specific assay of Akt activity in cell lysates. Anal Biochem 2002;305:32–9.

**35.** Marks MG, Shi J, Fry MO, et al. Effects of putative hydroxylated thalidomide metabolites on blood vessel density in the chorioallantoic membrane (CAM) assay and on tumor and endothelial cell proliferation. Biol Pharm Bull 2002;25:597–604.

**36.** Zhu J, Huang JW, Tseng PH, et al. From the cyclooxygenase-2 inhibitor celecoxib to a novel class of 3-phosphoinositide-dependent protein kinase-1 inhibitors. Cancer Res 2004;64:4309-18.

**37.** Salinas M, Lopez-Valdaliso R, Martin D, Alvarez A, Cuadrado A. Inhibition of PKB/Akt1 by C2-ceramide involves activation of ceramide-activated protein phosphatase in PC12 cells. Mol Cell Neurosci 2000; 15:156–69.

**38.** Schubert KM, Scheid MP, Duronio V. Ceramide inhibits protein kinase B/Akt by promoting dephosphorylation of serine 473. J Biol Chem 2000; 275:13330–5.

**39.** Obaya AJ, Sedivy JM. Regulation of cyclin-Cdk activity in mammalian cells. Cell Mol Life Sci 2002;59:126–42.

**40.** Sandal T. Molecular aspects of the mammalian cell cycle and cancer. Oncologist 2002;7:73–81.

**41.** Brown VD, Phillips RA, Gallie BL. Cumulative effect of phosphorylation of pRB on regulation of E2F activity. Mol Cell Biol 1999;19:3246–56.

**42.** Donnellan R, Chetty R. Cyclin E in human cancers. FASEB J 1999; 13:773–80.

**43.** Fesquet D, Labbe JC, Derancourt J, et al. The MO15 gene encodes the catalytic subunit of a protein kinase that activates cdc2 and other cyclin-dependent kinases (CDKs) through phosphorylation of Thr161 and its homologues. EMBO J 1993;12:3111–21.

**44.** Makitie AA, Chau M, Lim S, et al. Selective inhibition of cyclooxygenase 2 induces p27kip1 and skp2 in oral squamous cell carcinoma. J Otolaryngol 2003;32:226–9.

**45.** Hsu AL, Ching TT, Wang DS, Song X, Rangnekar VM, Chen CS. The cyclooxygenase-2 inhibitor celecoxib induces apoptosis by blocking Akt activation in human prostate cancer cells independently of Bcl-2. J Biol Chem 2000;275:11397–403.

**46.** Jones MK, Wang H, Peskar BM, et al. Inhibition of angiogenesis by nonsteroidal anti-inflammatory drugs: insight into mechanisms and implications for cancer growth and ulcer healing. Nat Med 1999;5: 1418–23.

**47.** Senderowicz AM. The cell cycle as a target for cancer therapy: basic and clinical findings with the small molecule inhibitors flavopiridol and UCN-01. Oncologist 2002;7:12–9.

**48.** Sato S, Fujita N, Tsuruo T. Interference with PDK1-Akt survival signaling pathway by UCN-01 (7-hydroxystaurosporine). Oncogene 2002; 21:1727–38.

**49.** Soh JW, Weinstein IB. Role of COX-independent targets of NSAIDs and related compounds in cancer prevention and treatment. Prog Exp Tumor Res 2003;37:261–85.

**50.** Saini SS, Gessell-Lee DL, Peterson JW. The cox-2-specific inhibitor celecoxib inhibits adenylyl cyclase. Inflammation 2003;27:79–88.

**51.** Fenwick SW, Toogood GJ, Lodge JP, Hull MA. The effect of the selective cyclooxygenase-2 inhibitor rofecoxib on human colorectal cancer liver metastases. Gastroenterology 2003;125:716–29.

Molecular Cancer Therapeutics

# Growth inhibitory effects of celecoxib in human umbilical vein endothelial cells are mediated through $G_1$ arrest via multiple signaling mechanisms

Ho-Pi Lin, Samuel K. Kulp, Ping-Hui Tseng, et al.

*Mol Cancer Ther* 2004;3:1671-1680.